

## Record Extrinsic Transconductance (2.45 mS/ $\mu\text{m}$ at $V_{DS} = 0.5$ V) InAs/In<sub>0.53</sub>Ga<sub>0.47</sub>As Channel MOSFETs Using MOCVD Source-Drain Regrowth

S. Lee<sup>1</sup>, C.-Y. Huang<sup>1</sup>, A. D. Carter<sup>1</sup>, D. C. Elias<sup>1</sup>, J. J. M. Law<sup>1</sup>, V. Chobpattana<sup>2</sup>, S. Krämer<sup>2</sup>, B. J. Thibeault<sup>1</sup>, W. Mitchell<sup>1</sup>, S. Stemmer<sup>2</sup>, A. C. Gossard<sup>2</sup>, and M. J. W. Rodwell<sup>1</sup>

<sup>1</sup>ECE Department, <sup>2</sup>Materials Department, University of California, Santa Barbara, CA 93106 USA,

Email: [sanghoon\\_lee@ece.ucsb.edu](mailto:sanghoon_lee@ece.ucsb.edu)

**Abstract:** We report InAs/In<sub>0.53</sub>Ga<sub>0.47</sub>As channel MOSFETs using source-drain regrown contact and surface digital etching. A device with 40 nm- $L_g$  shows 2.45 mS/ $\mu\text{m}$  extrinsic peak transconductance  $g_m$  at  $V_{DS} = 0.5$  V and 214  $\Omega\text{-}\mu\text{m}$   $R_{on}$ . A long-channel device ( $L_g = 510$  nm) exhibits 1.06 mS/ $\mu\text{m}$   $g_m$  at  $V_{DS} = 0.5$  V and 93 mV/dec at  $V_{DS} = 0.05$  V. At all gate lengths, the devices exhibit the highest extrinsic  $g_m$  among published results on III-V MOSFETs and MOSHEMTs.

**Introduction:** Due to the excellent electron transport properties, In<sub>x</sub>Ga<sub>1-x</sub>As-based MOSFETs have been widely investigated as promising candidates for future VLSI [1]-[7]. Among various design prototypes, substitutional-gate with source-drain (S/D) regrowth can be considered a viable design scheme at sub-10 nm node since it enables heavily-doped S/D regions without dry-etching of a gate metal stack, or “trench” etching with etch-stop layers. In such a device, however, performance can be degraded by damage to the channel surface during regrowth [8]. Here, we demonstrate InAs/In<sub>0.53</sub>Ga<sub>0.47</sub>As MOSFETs using MOCVD S/D regrowth and a substitutional-gate process. Employing surface digital etching [7]-[8], one can remove the damaged semiconductor surface and also control the channel thickness with nearly nanometer precision. The devices fabricated show the highest peak extrinsic transconductance ( $g_m$ ) at all gate lengths among reported III-V MOSFETs.

**Device Fabrication:** The epitaxial layers, grown on a semi-insulating InP substrate by molecular beam epitaxy, consist of the following: a 400 nm unintentionally doped In<sub>0.52</sub>Al<sub>0.48</sub>As buffer/barrier layer, a 3 nm Si-doped ( $3.9 \times 10^{12}$  cm<sup>-2</sup>) In<sub>0.52</sub>Al<sub>0.48</sub>As pulse doping layer, a 3 nm In<sub>0.53</sub>GaAs bottom cladding layer, a 5 nm InAs channel (strained), a 3 nm In<sub>0.53</sub>Ga<sub>0.47</sub>As top cladding and a 5 nm Si-doped ( $4\text{-}5 \times 10^{19}$  cm<sup>-3</sup>) In<sub>0.53</sub>Ga<sub>0.47</sub>As cap. To form dummy gates, 50 nm SiO<sub>2</sub> was deposited by PECVD and patterned by e-beam lithography and ICP dry etching. Immediately prior to loading into the MOCVD chamber for S/D regrowth, the surface was oxidized by UV ozone exposure and then etched in dilute HCl. 60 nm Si-doped ( $4 \times 10^{19}$  cm<sup>-3</sup>) In<sub>0.53</sub>Ga<sub>0.47</sub>As was selectively grown on the n<sup>+</sup> cap layer. Device mesas were defined by wet-etching, and the dummy gates removed in buffered oxide etch (BOE). The exposed n<sup>+</sup> cap and upper cladding layer were etched through multiple cycles of UV ozone exposure as oxidation and dilute HCl dip as surface oxide removal [8]-[10]. Immediately after removing the InGaAs surface oxide from the last cycle of UV ozone exposure in BOE, the sample was transferred into the ALD chamber, pre-cleaned/passivated by a cyclic N<sub>2</sub> plasma and TMA *in-situ* treatment, and subsequently  $\sim 3.6$  nm HfO<sub>2</sub> gate dielectric deposited [11]. The sample was then annealed for 15 minutes at 400 °C in forming gas. 20 nm/100 nm Ni/Au was thermally deposited as the gate electrode. Subsequently, 20 nm/100 nm Ti/Pd/Au was lifted off for source/drain metallization. Fig. 1 shows a schematic cross-section of the device.

**Results and Discussion:** Fig. 2 shows a cross-sectional STEM for a 40 nm- $L_g$  device. The HR-TEM inset of Fig. 2 confirms that  $\sim 0.5$  nm interfacial layer is formed by N<sub>2</sub> plasma and TMA treatment and the channel of the device has 5 nm InAs, which is not relaxed, and 3 nm In<sub>0.53</sub>Ga<sub>0.47</sub>As. Fig. 3 shows a simulation of the energy band structure and the charge density at  $V_{GS} = 0.5$  V by 1D Poisson-Schrödinger solver. The transfer characteristics of short channel devices are shown in Fig. 4. The devices with 40, 70, and 90 nm- $L_g$  show 2.45, 2.40 and 2.16 mS/ $\mu\text{m}$  peak extrinsic  $g_m$  at  $V_{DS} = 0.5$  V, respectively. All chips on the test sample (30 dies) show a similar performance (<10% variability). Fig. 5 shows the output characteristics of a 40 nm- $L_g$  device. Its maximum drain current density is 1.95 mA/ $\mu\text{m}$  at  $V_{GS} = 1.4$  V and  $V_{DS} = 0.5$  V and its on-resistance is 214  $\Omega\text{-}\mu\text{m}$ . Fig. 6 shows the subthreshold characteristics of short channel devices. The subthreshold swings (SS) of devices with 40, 70, 90 nm- $L_g$  are  $\sim 155$ , 115 and 110 mV/dec at  $V_{DS} = 0.05$  V and  $\sim 400$ , 235, and 190 mV/dec at  $V_{DS} = 0.5$  V, respectively. The gate leakage current is negligible,  $< 10^{-3}$  A/cm<sup>2</sup> at all gate biases measured, as shown in the inset of Fig. 6. The transfer and subthreshold characteristics of a long channel ( $L_g = 510$  nm) device are shown in Fig. 7. The device shows 1.05 peak extrinsic  $g_m$  at  $V_{DS} = 0.5$  V and the minimum SS of  $\sim 93$  mV/dec at  $V_{DS} = 0.05$  V. From transmission line method (TLM) measurements, shown in Fig. 9, 4.7  $\Omega\text{-}\mu\text{m}^2$  S/D metal contact resistivity and  $\sim 25$   $\Omega$ /square sheet resistance of the regrown S/D contact layer are extracted. Considering the gap between S/D metal contact and the channel, shown in inset of Fig. 9, S/D access resistance ( $R_{SD}$ ) is determined to be  $\sim 82$   $\Omega\text{-}\mu\text{m}$ , which degrades  $g_m$  by  $\sim 8\%$ . Fig. 9 shows dependency of SS and threshold voltage, which was extracted from linear extrapolation, against gate length. The devices with short  $L_g$ , less than 100 nm, exhibit poor short channel effects, which may be attributed to back-barrier conduction due to heavy pulse doping. Fig. 10 shows  $R_{on}$  in terms of gate length. Despite a relatively large gap between the S/D metal and the channel ( $\sim 1.2$   $\mu\text{m}$  for each side) due to non-self-aligned S/D metal contacts, the device shows very low  $R_{on}$  at all gate lengths. As a benchmark, Fig. 11 compares extrinsic peak  $g_m$  versus  $L_g$  with other published III-V MOSFETs and MOSHEMTs. This result is the best III-V MOSFET/MOSHET extrinsic  $g_m$  at all gate lengths at a given low supply voltage ( $V_{DS} = 0.5$  V), almost equaling that of InAs HEMTs.

**Conclusion:** We have demonstrated InAs/In<sub>0.53</sub>Ga<sub>0.47</sub>As channel MOSFETs using MOCVD regrown S/D and surface digital etching. The device with 40 nm- $L_g$  shows excellent on-state performance of 2.45 mS/ $\mu\text{m}$  peak extrinsic  $g_m$  at  $V_{DS} = 0.5$  V.

**Acknowledgement:** This work was supported by the SRC Non-classical CMOS Research Center (Task 1437.009). A portion of this work was done in the UCSB Nanofabrication facility, part of the NSF funded NNIN network and MRL Central Facilities supported by the MRSEC Program of the NSF under award No. DMR 1121053.

**References:** [1] M. Radosavljevic *et al.*, IEDM, p.319 (2009), [2] D.-H. Kim *et al.*, IEDM, p. 761 (2012), [3] T.-W. Kim *et al.*, VLSI, p. 179 (2012), [4] J. J. Gu *et al.*, IEDM, p. 633 (2012), [5] M. Egard *et al.*, IEDM, p. 303 (2011), [6] Y. Yonai *et al.*, IEDM, p. 307 (2011), [7] J. Lin *et al.*, IEDM, p. 757 (2012), [8] S. Lee *et al.*, IPRM, accepted (2013), [9] R. Driad *et al.*, IPRM, p.459 (1998), [10] J. R. Vig. JVST May/June p. 1027 (1985) [11] V. Chobpattana *et al.*, APL p.102, 022907 (2013)

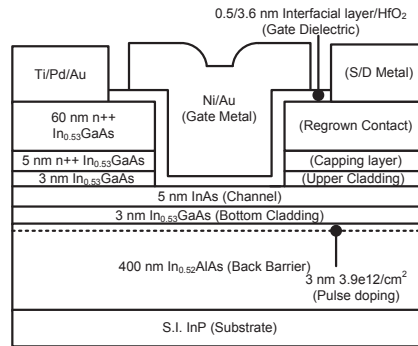


Fig. 1. Schematic cross-section of InAs/In<sub>0.53</sub>GaAs MOSFET with MOCVD S/D regrowth and surface recess etching.

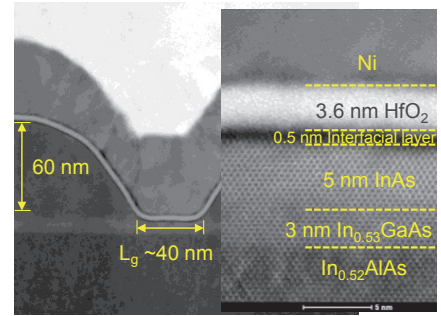


Fig. 2. Cross-sectional STEM of a 40 nm- $L_g$  device.  $\sim 0.5$  nm interfacial layer,  $\sim 3.6$  nm HfO<sub>2</sub> and 5/3 nm InAs/In<sub>0.53</sub>GaAs channel.

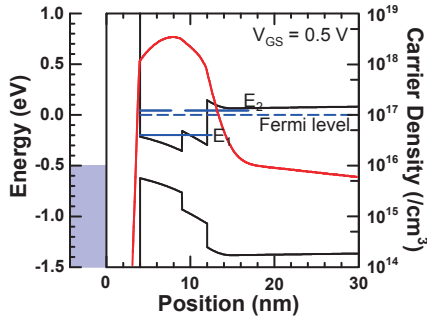


Fig. 3. Energy band structure and charge distribution at  $V_{GS} = 0.5$  V by 1D Poisson-Schrödinger simulation.

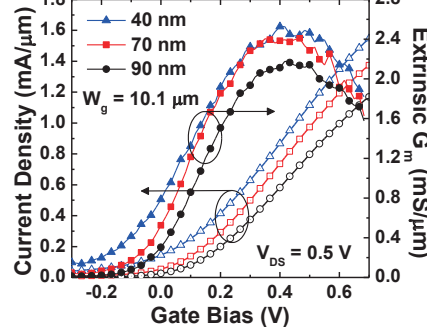


Fig. 4. Transfer characteristics of short channel devices (40/70/90 nm- $L_g$ ).

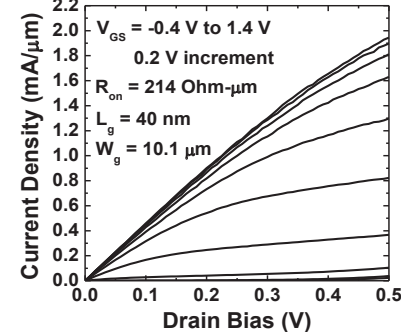


Fig. 5. Output characteristics of a 40 nm- $L_g$  device.

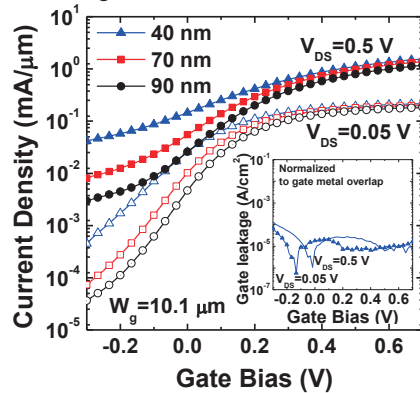


Fig. 6. Subthreshold characteristics of short channel devices (40/70/90 nm- $L_g$ ) and gate leakage current for the 40 nm- $L_g$  device.

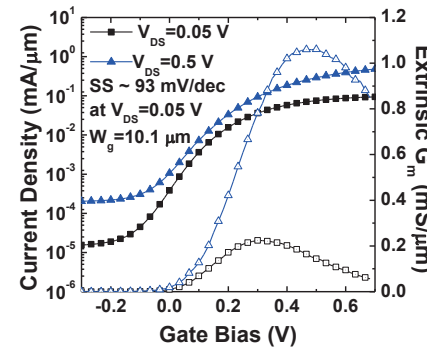


Fig. 7. Subthreshold characteristics of a 510 nm- $L_g$  channel device. The minimum SS is  $\sim 93$  mV/dec at  $V_{DS} = 0.05$  V.

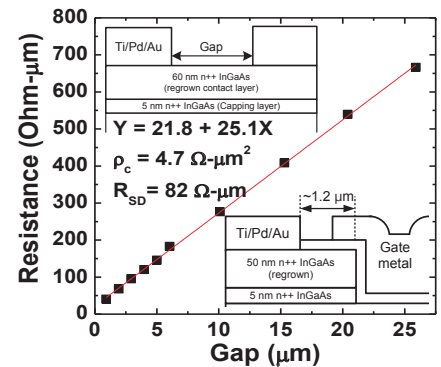


Fig. 8. TLM measurements of the regrown S/D contact layer.

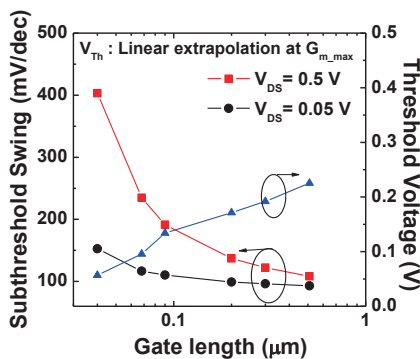


Fig. 9. Subthreshold Swing with respect to the gate length for  $V_{DS} = 0.05$  V and 0.5 V.

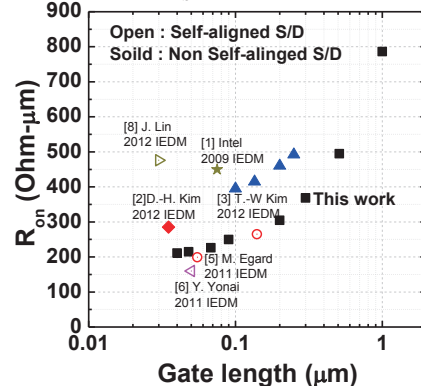


Fig. 10. On-resistance ( $R_{on}$ ) with respect to the gate length.  $R_{on}$  is very low, particularly given the non-self-aligned S/D contacts.

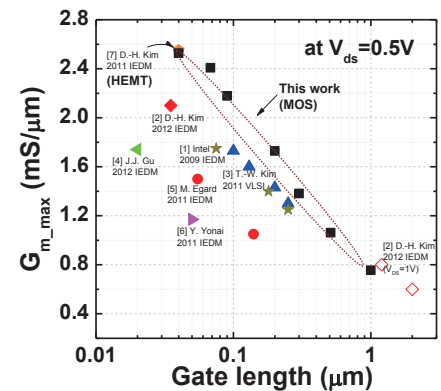


Fig. 11. Peak extrinsic  $g_m$  vs. gate length for III-V MOSFETs and MOSHEMTs. Data for a record HEMT is also shown.